Responses to Reviewers:

Reviewer 1:

We thank the reviewer for the careful reading of the manuscript and helpful comments. We have revised the manuscript following their suggestions as is described below.

This study could be a very meaningful work. The paper addressed the relevant scientific questions within the scope of ACP. This manuscript studied the possible reasons enhancing the ozone formation under high PM2.5 concentrations. It is not a very novel concept since some previous studies already reported the positive correlation between PM2.5 and ozone, and analyzed the underestimated HONO sources in China and other areas in the world. However, better understanding the mechanisms in different locations is scientifically significant in modeling studies. In addition, as the authors mentioned, the results bring important insights for control strategy of air pollution, be- cause both PM2.5 and ozone are significant air pollutants in China.

There sever major concerns as follows:

(1) Both cloud and aerosol can affect the solar radiation. In order to separate these two factors, especially for case studies, people usually will analyze the meteorological conditions during the measurement period, or only analyze the data under the cloud- free conditions. However, the authors of this manuscript never mentioned the cloud factor.

Thanks for the valuable comments of the reviewer. We have checked the meteorological condition (especially cloud condition) during the period of the case study (between Oct 5 and 6, 2015) in the Beijing region. It shows that there was close to the cloud free condition (see attached Fig-A1. Now it is Fig. 5 in the revised paper). In order to evaluate the effect of cloud, we made additional model runs (with thing and thick cloud conditions). The results show that clouds have important impact on the result of this study, and this study is more suitable for the cloud free conditions (see attached Fig-A2. Now it is Fig. 12 in the revised paper). The results show that the thin cloud (cloud cover in 2 km, with cloud water of 10 g/m^3), could reduce the photolysis rate of HONO by about 40%, but the HONO could still remain important effects. However, with dense cloud condition (cloud covers at 2 and 3 km, with cloud water of 50 10 g/m^3), the photolysis rate of HONO could reduce by 9-10 times by the cloud. In this case, adding photolysis rate of HONO cannot produce important effect on OH radicals and the production of O_3. The above statements have been added in the revised manuscript.

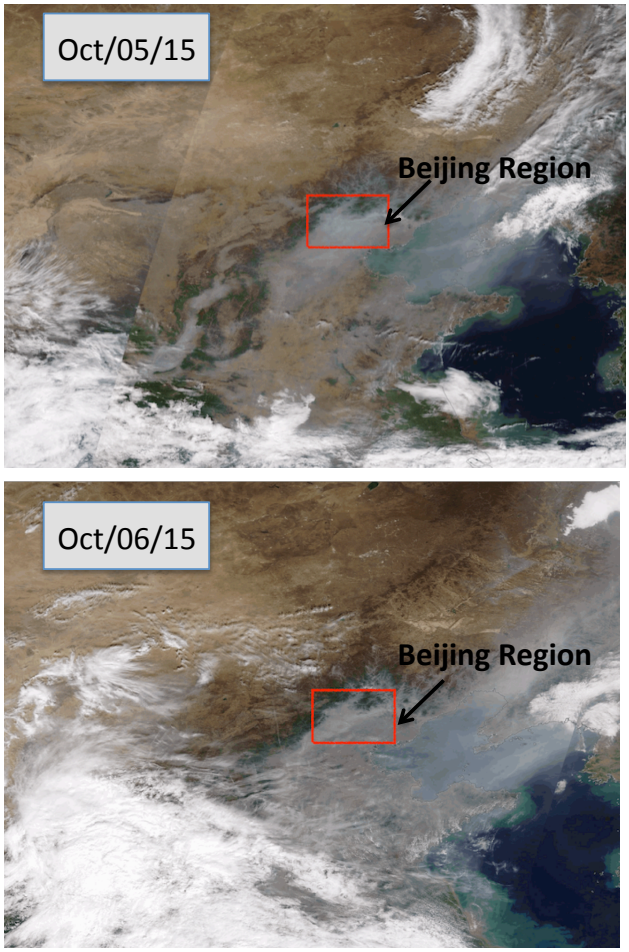

Fig-A1. The cloud condition during the period of the case study (between Oct 5 and 6, 2015 in the Beijing region. The bright white color shows the cloud covers, and the grey white shows the haze covers. The Beijing region is under the heavy haze conditions during the period.

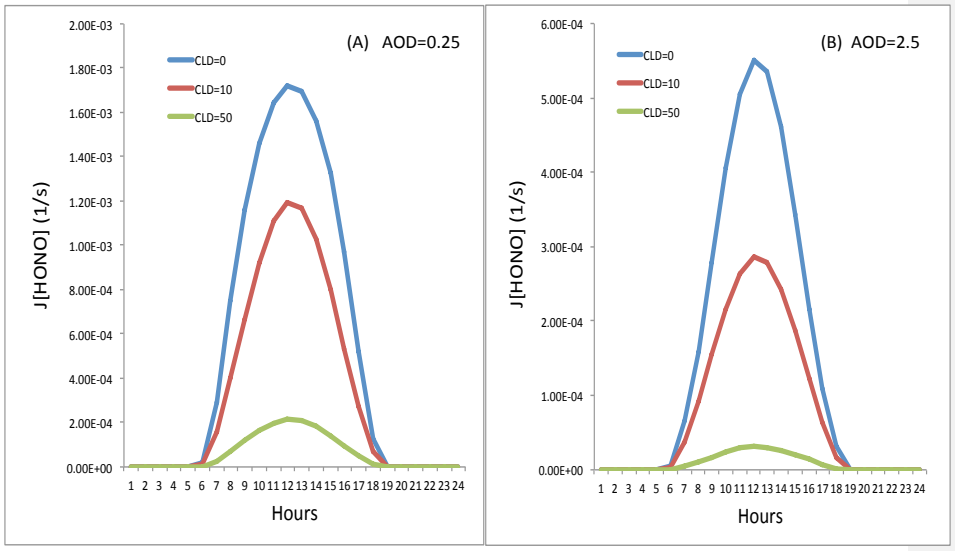

Fig-A2. The effect of cloud cover on the photolysis rate of HONO (J[HONO]). The blue, red, and green lines represent the cloud water vapor of 0 (cloud-free), 10 (g/m^3 – thin cloud), and 50 (g/m^3 – thick cloud), respectively. The left panel (A) represents the light aerosol condition, with AOD of 0.25, and the right panel (B) represents the heavy aerosol condition, with AOD of 2.5.

(2) Several important previous studies should be mentioned so that some conclusions from this manuscript can be more solid. For example (but not limited to), Zhang et al. (2016) already parameterized up-to-date HONO sources into WRF-Chem model such as the heterogeneous reactions on ground and aerosol surfaces, direct vehicle and vessel emissions, conversion of NO2 at the ocean surface, and emissions from soil bacteria. The modified WRF-Chem substantially reproduced the observed HONO levels, and greatly improved the ozone simulations. However, in this manuscript, the calculated HONO level was still very low in Fig. 6. More information about the WRF- Chem setup is needed. In addition, some other studies (e.g., Shi et al., 2015) already reported the positive correlation between aerosol and ozone. The ozone formation is also strongly dependent on the aerosol size and composition. The process might be a complex interaction between aerosols and photochemical reactions. For example, the scattering aerosol could considerably diffuse the solar radiation and enhance the flux density inside the boundary layer (He and Carmichael, 1999). Thus, the scattering aerosols may favor the ozone formation through increasing solar flux in the boundary layer (Shi et al., 2015). More discussions are needed in the manuscript.

Thanks for the valuable comments of the reviewer. We think that adding these previous studies will enhance the understanding of the highlights of our paper. The reviewer points that some recent versions of the WRF-Chem model add some missing HONO sources (surface emissions, conversion of NO_2 at the ocean surface, etc.) can improve the HONO calculations (Shi et al., 2015). In our calculation, we only use the classical gas-phase

chemistry to illustrate that the importance of these missing sources for the production of OH radicals. Adding these missing sources (there are not fully understand and remain a large uncertainty) could be a future work. In the revised paper, we add the above clarifications. We also add the reference of He and Carmichael (1999) to add their point that there maybe another factor that the ratio of the scattering and absorbing aerosols could be another factor to affect the relationship between aerosols and ozone. All the valuable references are included in the revised paper.

Zhang, L., Wang, T., Zhang, Q., Zheng, J., Xu, Z., & Lv, M. (2016). Potential sources of nitrous acid (HONO) and their impacts on ozone: A WRF/Chem study in a polluted subtropical region. Journal of Geophysical Research: Atmospheres, 121(7), 3645- 3662.

Shi, C., Wang, S., Liu, R., Zhou, R., Li, D., Wang, W., ... & Zhou, B. (2015). A study of aerosol optical properties during ozone pollution episodes in 2013 over Shanghai, China. Atmospheric Research, 153, 235-249.

He, S., & Carmichael, G. R. (1999). Sensitivity of photolysis rates and ozone pro- duction in the troposphere to aerosol properties. Journal of Geophysical Research: Atmospheres, 104(D21), 26307-26324.

Generally, this manuscript presents a significant study; however, the analysis should be in more depth. The authors should give proper credit to related work, and clearly indicate this manuscript's original contribution. I would not recommend using a vague word (such as "low solar radiation") in the title.

Thanks. We change title from "Ozone formation under low solar radiation in eastern China" to "Ozone enhancement due to photo-disassociation of nitrous acid in eastern China"

Responses to Reviewers:

Reviewer 2:

We thank the reviewer for the careful reading of the manuscript and helpful comments. We have revised the manuscript following their suggestions as is described below.

This work tried to explain the measured co-occurrence of high PM2.5 and O3 concentrations. The authors report that the high daytime HONO concentrations could be photo-dissociated to be OH radicals, which enhance the photochemical production of O3, although depressed solar radiation under heavy PM2.5 pollutions. It is an interesting scientific issues. However, the data and method in the manuscript do not support such a conclusion very well at this stage.

My major concerns are listed as follows:

(1) The authors mixed observations from Shanghai and Beijing to create an illusion. There are no observations to show high PM2.5-O3-HONO concentrations both at Shanghai and at Beijing. I just see high PM2.5-O3 during Oct.5-6, 2015 in Beijing and high PM2.5-HONO during September, 2009 in Shanghai.

Thanks for pointing out this issue. The reason we chose the data by the following reasons. (1) Because the co-occurrence between O3 and PM2.5 are not always happened, it happens only in some episodes, especially in spring and fall. In winter, O3 and PM2.5 are actually anti-correlated due to low solar radiation (This also can see in Fig. 2 of the paper). It occurs under the following condition, (a) under cloud-free condition, (b) solar radiation is not too low, (c) during heavy aerosol pollutions in large cities in eastern China. Due to these limitations, it requires continuously measurements of O3 and PM2.5, and HONO concentrations. Recently, there are some continuously measurements of PM2.5, and O3 concentrations released by EPA of China. However, HONO measurements are not continuously measured, and we cannot find the HONO data with the period of co-occurrence between O3 and PM2.5. However, we do find some HONO measurements, which all shows that in all major Chinese cities in either fall or winter (Shanghai, Beijing, and Xian), the HONO concentrations were significant higher than other regions (see attached Fig-A1; Now in Fig. 8 of revised paper). For example, HONO concentrations reached highest in night, ranging from 1 to 2.5 ppbv in the morning at 6-9am. In daytime, the concentrations were lowest (ranging from 0.3 to 1.0 ppbv at12-18pm), but the concentrations were still significant higher than other regions, which could have significant effect on the production of OH radicals in daytime. As a result, we think that the high HONO is a common event in large cities in eastern China, especially in daytime. This high daytime high HONO is supported by the measurements in previous studies (Zhang et al. 2016; Huang et al. 2017). In this study, we make an assumption that the co-occurrence between O3 and PM2.5 occurred under high HONO concentrations. From Fig.-A1, we also note that using this assumption may result in some uncertainties in estimating the effect of HONO on OH. For example, using the measured HONO in Xi'an

and Beijing could produce 1-2 times higher OH production by photolysis of HONO than the result by using the measured data from Shanghai. In this case, we use the measured HONO from Shanghai to avoid the over estimate of the HONO effect, which can be considered as a low-limit estimation. The above statements are added in the revised paper.

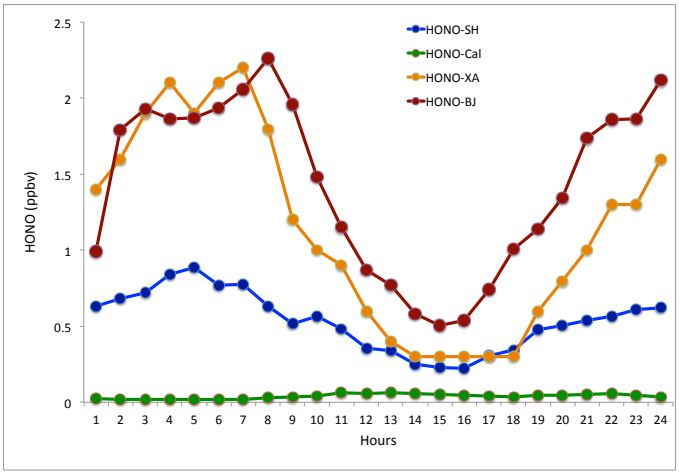

Fig. A1. The measured HONO concentrations (ppbv) in three large cities in China. The red line was measured in Xi'An from 24 July to August 6, 2015. The blue line was measured in Shanghai from 9 to 18 September, 2009. The dark-red line was measured in Beijing from 1 to 27 January, 2014. The green line is calculated by the WRF-Chem model. The measurement in fall of Shanghai is applied to the calculation for the OH production of HONO.

(2) Is the observed co-occurrence of high PM2.5 and O3 concentrations of statistical significance? Are the authors sure it's (measurements during Oct.5-6) not a special case?

The co-occurrence of high PM2.5 and O3 concentrations was occurred in several cases in the past years. The attached Fig.-A2 shows some examples. Because it happened under some special conditions (see the reply in question 1), it most occurred in spring and fall seasons.

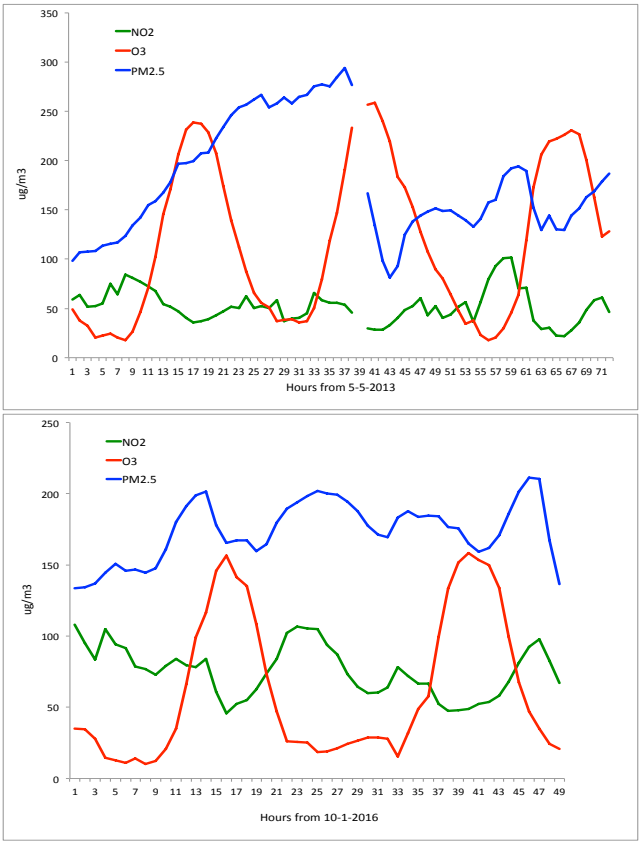

Fig.-A2. The diurnal variations of $PM_{2.5}$ (blue line) and O_3 (red line), and NO_2 (green line) during the periods (from May 5 to May 7, 2013 (upper panel) and from Oct. 1 to Oct. 2, 2016 (lower panel)).

(3) Could the authors make an effort to exclude the effects of precursor emissions (e.g., being sure that the VOCs/NOx ratios are not more beneficial for ozone production during Oct.5-6 than other days) and meteorological conditions (e.g., temperature and relative humidity; under low humidity, although the PM2.5 concentration is high, the solar radiation would not be depressed much)? Moreover, there are no observations show the solar radiation are exactly depressed during Oct.5-6 in Beijing or September in Shanghai?

Thanks for the valuable comments. We tried to find the available data, which is available during the period of Oct. 5 to 6, 2015. We do find some interesting data, which could answer the some comments of the reviewer. The additional data also helps to improve the quality of the paper. Fig.-A3 (now Fig. 5 in the revised paper) shows the cloud conditions in Beijing. During the period, there was close to the cloud free condition，but there was a very heavy aerosol layer. Fig.-A4 shows the relative humidity (RH) conditions. It shows that the RH (%) was generally higher than

60%, with a maximum of 95% during the period. As a result, the high aerosol concentrations companied by high RH produced important effects on solar radiation. As shown in Fig.-A5 (now Fig. 6 in revised paper), the daytime averaged solar radiation was significantly reduced (about 40% reduction in Oct. 5-6 compared with the value of Oct. 8). We thanks the comments by the reviewer, these addition (figures and text) can significant enhance the quality of the paper.

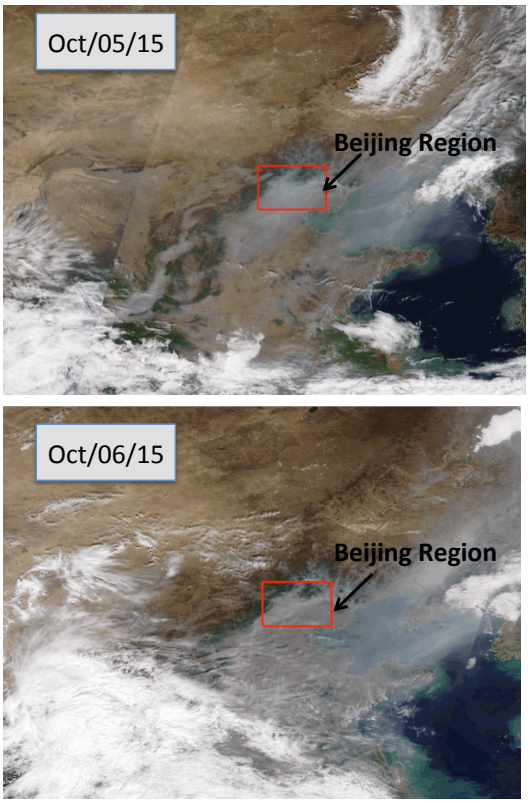

Fig-A3. The cloud condition during the period of the case study (between Oct 5 and 6, 2015 in the Beijing region. The bright white color shows the cloud covers, and the grey white shows the haze covers. The Beijing region is under the heavy haze conditions during the period.

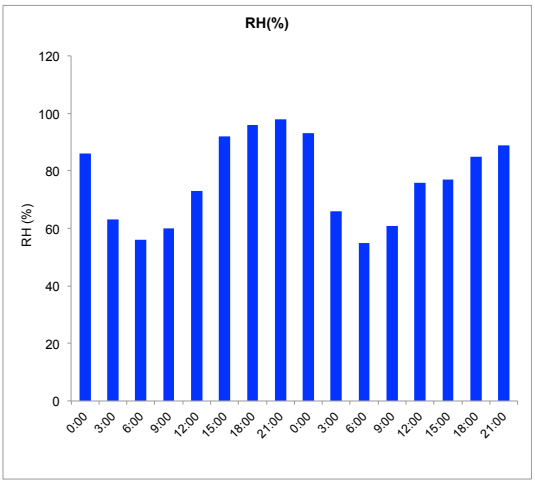

Fig-A4. The measured relative humidity (RH) conditions between Oct. 5 and Oct.6, 2015.

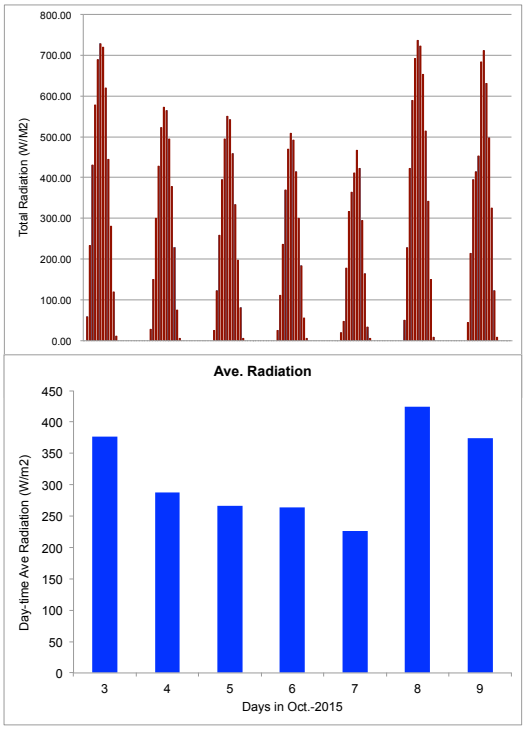

Fig-A5. The measured solar radiation (W/m^2) from Oct. 3 to Oct. 9, 2015 in Beijing. The upper panel shows hourly values, and the lower panel shows the daytime averaged values.

(4) If the authors insist the high PM2.5-O3-HONO mechanism, could this possible new mechanism be added to the WRF-Chem model for verification?

Adding the high PM2.5-O3-HONO mechanism is a very challenge work, and could be another

scientific work in the future. The major difficulty is that the causes (surface emissions or chemical transformations?) for the high HONO concentrations in large Chinese cities are not clearly understood. This could be a very interesting work in the future.

(5) Discussion in sect.3.3: the conclusion (solar radiation in winter reaches a threshold level to prevent the OH chemical production, even by including the HONO production term) came too hastily without no direct evidence.

Thanks for the comment. We agree with the reviewer that this conclusion is not very certain, and we re-write these sentences to soft the tone of this conclusion. In the revised paper, we change "When the solar radiation is in a very low level in winter, it reaches the threshold level to prevent the OH chemical production, even by including the HONO production of OH." to "Because the solar radiation is in a very low level in winter, adding the photolysis of HONO has smaller effect in winter than in fall, and OH remains low values by including the HONO production term."

Specific comments:

(1) L167-169: there are no data to show the solar radiation are reduced
We add a new figure and text to show the solar reduction.

(2) L185: same above
Answered in the above.

(3) L188-190: same above
Answered in the above.

(4) L199: "Chine" should be "China"
Corrected.

(5) L201: removed "OH"
Corrected.

(6) L218: what is "am" in O1D + am->O3P
am represents air mass in chemical reaction equations.

(7) L222: "Madronich and Flocke (1999)" should be "(Madronich and Flocke, 1999)"
Corrected.

(8) L295-296: one of "P1" should be "P2"?
Corrected.

(9) L298-299: one of "P1" should be "P2" ? (10) L241: What are possible sources of HONO?
Corrected. The possible sources of HONO could be surface sources or heterogeneous chemical reactions (but they are not fully understood at present).

Reference:

Zhang, L., Wang, T., Zhang, Q., Zheng, J., Xu, Z., & Lv, M. (2016). Potential sources of nitrous acid (HONO) and their impacts on ozone: A WRF/Chem study in a polluted subtropical region. Journal of Geophysical Research: Atmospheres, 121(7), 3645- 3662.

Huang, R. J., L. Yang, JJ Cao, QY Wang, X. Tie, et al., Concentration and sources of atmospheric nitrous acid (HONO) at an urban site in Western China. *Sci. of Total Environ*., 593-594, 165-172, doi.org/10.1016/j.scitotenv.2017.02.166, 2017.

Ozone enhancement due to photo-disassociation of nitrous acid in eastern China

Xuexi Tie[1,2], Xin Long[1,5], Guohui Li[1], Shuyu Zhao[1], Jianming Xu[3,4]

[1] KLACP, SKLLQG, Institute of Earth Environment, Chinese Academy of Sciences, Xi'an 710061, China

[2]Center for Excellence in Urban Atmospheric Environment, Institute of Urban Environment, Chinese Academy of Sciences, Xiamen 361021, China

[3] Shanghai Meteorological Service, Shanghai, 200030, China

[4]Shanghai Key Laboratory of Meteorology and Health, Shanghai, 200030, China

[5]School of Environment Science and Engineering, Southern University of Science and Technology, Shenzhen 518055, China

Correspondence to: XueXi Tie (tiexx@ieecas.cn) or Jianming Xu (metxujm@163.cn)

XUEXI TIE 3/7/19 2:46 PM
已设置格式: 字体:18 pt, 加粗

XUEXI TIE 3/7/19 2:46 PM
已设置格式: 字体:18 pt

XUEXI TIE 3/7/19 2:46 PM
已删除: **Ozone formation under low solar radiation in eastern China**

XUEXI TIE 10/7/19 9:36 AM
已设置格式: 上标

XUEXI TIE 10/7/19 9:35 AM
已删除:

XUEXI TIE 10/7/19 9:35 AM
已设置格式: 字体:10 pt

Abstract

$PM_{2.5}$, a particulate matter with a diameter of 2.5 micrometers or less, is one of the major components of the air pollution in eastern China. In the past few years, China's government made strong efforts to reduce the $PM_{2.5}$ pollutions. However, another important pollutant (ozone) becomes an important problem in eastern China. Ozone (O_3) is produced by photochemistry, which requires solar radiation for the formation of O_3. Under heavy $PM_{2.5}$ pollution, the solar radiation is often depressed, and the photochemical production of O_3 is prohibited. This study shows that during fall in eastern China, under heavy $PM_{2.5}$ pollutions, there were often strong O_3 photochemical productions, causing a co-occurrence of high $PM_{2.5}$ and O_3 concentrations. This co-occurrence of high $PM_{2.5}$ and O_3 is un-usual and is the main focus of this study. Recent measurements show that there were often high HONO surface concentrations in major Chinese mega cities, especially during daytime, with maximum concentrations ranging from 0.5 to 2 ppbv. It is also interesting to note that the high HONO concentrations were occurred during high aerosol concentration periods, suggesting that there were additional HONO surface sources in eastern China. Under the high daytime HONO concentrations, HONO can be photo-dissociated to be OH radicals, which enhance the photochemical production of O_3. In order to study the above scientific issues, a radiative transfer model (TUV; Tropospheric Ultraviolet-Visible) is used in this study, and a chemical steady state model is established to calculate OH radical concentrations. The calculations show that by including the OH production of the photo-dissociated of HONO, the calculated OH concentrations are significantly higher than the values without including this production. For example, by including HONO production, the maximum of OH concentration under the high aerosol condition (AOD=2.5) is similar to the value under low aerosol condition (AOD=0.25) in the no-HONO case. This result suggests that even under the high aerosol condition, the chemical oxidizing process for O_3 production can occurred, which explain the co-occurrence of high $PM_{2.5}$ and high O_3 in spring and fall seasons in eastern China. However, the O_3 concentrations were not

significantly affected by the appearance of HONO in winter. This study shows that the seasonal variation of solar radiation plays important roles for controlling the OH production in winter. Because the solar radiation is in a very low level in winter, adding the photolysis of HONO has smaller effect in winter than in fall, and OH remains low values by including the HONO production term. This study provides some important scientific highlights to better understand the O_3 pollutions in eastern China.

Keywords; High $PM_{2.5}$ and O_3, eastern China, HONO photolysis

XUEXI TIE 9/7/19 4:50 PM

已删除: When the solar radiation is in a very low level in winter, it reaches the threshold level to prevent the OH chemical production, even by including the HONO production of OH.

1. Introduction

Currently, China is undergoing a rapid economic development, resulting in a higher demand for energy and greater use of fossil fuels. As a result, the high emissions of pollutants produce heavy pollutions in mega cities of eastern China, such as Beijing and Shanghai. For example, in the city of Shanghai (a largest mega city in China), the urban and economical developments of the city are very rapid. During 1990 to 2015, the population increased from 13.3 to 24.1 million. The number of automobiles increased from 0.2 million (1993) to 2.0 million (2011). The rapid growing population and energy usage caused a rapid increase in the emissions of pollutants, leading to severe air pollution problems in these mega cities (Zhang et al., 2006; Geng et al., 2007; Deng et al., 2008).

Measurements, such as satellite observations have revealed much higher aerosol pollution in eastern China than in eastern US (Tie et al., 2006). The high aerosol pollution causes a wide range of environmental consequences. According to a study by Tie et al. (2009a), exposure to extremely high particle concentrations leads to a great increase of lung cancer cases. High PM (particular matter) concentrations also significantly reduce the range of visibility in China's mega cities (Deng et al., 2008). According to a recent study, the high aerosol pollution causes important effects on the crop (rice and wheat) production in eastern China (Tie et al., 2016).

In the troposphere, ozone formation is resulted from a complicated chemical process, and requires ozone precursors, such as VOCs (volatile organic carbons) and NO_X = $NO + NO_2$ (nitrogen oxides) (Sillman, 1995). As the increase in industrial activity and number of automobiles, the precursors of ozone (O_3) and the global budget of oxidization are also significantly increased (Huang et al., 2017; Huang et al., 2018). As a result, O_3 pollutions are becomes a serous pollution problem in Shanghai and other Chinese mega cities (Geng et al., 2010; Tie 2009b; Tie et al., 2015). The effects on O_3 production rate can be characterized as either NO_X-sensitive or VOC-sensitive conditions (Sillman, 1995; Zhang et al., 2003; Lei et al., 2004; Tie et al., 2013). Thus, better understanding the trends of O_3 precursors (VOCs, NO_X) is important to

determine the O_3 trends in Shanghai (as well as many large cities in China).

In the past few years, China's government made strong efforts to reduce the $PM_{2.5}$ pollutions. However, another important pollutant (O_3) becomes an important problem in eastern China. Several studies regarding the O_3 formation are previously studied in Shanghai. For example, Geng et al. (2007; 2008) study the relationship between O_3 precursors (NOx and VOCs) for the ozone formation in Shanghai. Tie et al. (2009) study the short-term variability of O_3 in Shanghai. Their study suggested that in addition to the ozone precursors, meteorological conditions, such as regional transport, have also strong impacts on the ozone concentrations. During September 2009, a major field experiment (the MIRAGE-Shanghai) was conducted in Shanghai, and multiply chemical species were measured during the experiment. The summary of the measurements by Tie et al (2013) suggests that the ozone formation in Shanghai is under VOC-sensitive condition. However, if the emission ration of NOx/VOCs reduces to a lower value (0.1-0.2), the ozone formation in Shanghai will switch from VOC-sensitive condition to NOx-sensitive condition.

Despite of some progresses have been made for the ozone formation in mega cities in China, it is still lack of study of ozone development in large cities of China. For example, this study shows that during fall in eastern China, under heavy $PM_{2.5}$ pollutions, there were often strong O_3 chemical productions, causing the co-occurrence of high $PM_{2.5}$ and O_3 concentrations. Under heavy aerosol condition, the solar radiation is depressed, significantly reducing the photochemical production of O_3. This co-occurrence of high $PM_{2.5}$ and O_3 is an unusual and is the focus of this study. He and Carmichael (1999) suggest that aerosol particles can enhance the scattering of solar radiation, enhancing the flux density inside the boundary layer. Recent measurements also show that there were often high HONO concentrations in major Chinese mega cities, especially during daytime, with maximum concentrations ranging from 0.5 to 2 ppbv (Huang et al., 2017). Shi et al. (2015) suggest that there are several potential HONO sources, including surface emissions, conversion of NO_2 at the ocean surface, etc., and adding these sources can improve the calculated HONO

XUEXI TIE 4/7/19 10:00 AM
已设置格式: 字体:12 pt

XUEXI TIE 4/7/19 9:53 AM
已设置格式: 字体:12 pt

concentrations. It is also interesting to note that the high HONO surface concentrations were occurred during high aerosol concentration periods, suggesting that there are additional HONO surface sources in eastern China. Under the high daytime HONO concentrations, HONO can be photo-dissociated to be OH radicals, which enhance the photochemical production of O_3.

The paper is organized as follows: in Section 2, we describe the measurement of O_3 and $PM_{2.5}$. In Section 3, we describe the calculation of photo-dissociated rate of HONO and a steady state model for the calculation of OH, and the causes of high O_3 production under the heavy aerosol condition. Section 4 shows a brief conclusion of the results.

XUEXI TIE 10/7/19 9:25 AM
已设置格式: 下标

XUEXI TIE 10/7/19 9:25 AM
已设置格式: 下标

XUEXI TIE 10/7/19 9:25 AM
已设置格式: 下标

2. Measurements of O_3 and $PM_{2.5}$

There are long-term measurements in Eastern China by Chinese Environment Protection Agency (CEPA) for monitoring the air quality in China. In eastern China, especially in the capital city of China (Beijing), there are often heavy air pollutions, especially for fine particular matter ($PM_{2.5}$ – the radium of particle being less than 2.5 um). Figure 1 shows the measurement sites in Beijing, in which the measured concentrations of $PM_{2.5}$ and O_3 are used to the analysis. In the region, the air pollutions were very heavy, especially in winter (Long et al., 2016; Tie et al., 2017). The previous studies suggested that the both aerosol and O_3 pollutions became the major pollutants in the region (Li et al., 2017).

Figure 2 shows the daily averaged concentrations of $PM_{2.5}$ and O_3 in the Beijing region in 2015. The daily averaged concentrations show that there were strong daily and seasonal variations for both the concentrations of $PM_{2.5}$ and O_3. Despite the daily variation, the concentrations of $PM_{2.5}$ existed a strong seasonal variation. For example,

there were very high concentrations during winter, with maximum of ~300 $\mu g/m^3$. While in summer, the maximum concentrations reduced to ~150 $\mu g/m^3$. The seasonal variability of O_3 concentrations were opposite with the $PM_{2.5}$ concentrations, with lower concentrations in winter (< 50 μg /m^3) and higher concentrations in summer (> 150 $\mu g/m^3$). These seasonal variations of $PM_{2.5}$ and O_3 have been studied by previous studies (Tie and Cao, 2017; Li et al., 2017). Their results suggest that the winter high $PM_{2.5}$ concentrations were resulted from the combination of both the high emissions (heating season in the Beijing region), and poor meteorological ventilation conditions, such as lower PBL (Planetary Boundary Layer) height (Quan et al., 2013; Tie et al. 2015). According to the photochemical theory of O_3 formation, the summer high and winter low O_3 concentrations are mainly due to seasonal variation of the solar radiation (Seinfeld, J. H. and Pandis, 2006).

In addition to the seasonal variation of solar radiation, the heavy aerosol concentrations play important roles to reduce solar radiation, causing the reduction of solar radiation and O_3 formation (Bian et al., 2007). As we show in Fig. 3a, during wintertime, the O_3 concentrations were strong anti-correlated with the $PM_{2.5}$ concentrations, suggesting that the reduction of solar radiation by aerosol particles have important impact on the reduction of O_3 concentrations. Figure 3a also shows that the relationship between O_3 and $PM_{2.5}$ was not linearly related. For example, when the concentrations of $PM_{2.5}$ were less than 100 $\mu g/m^3$, O_3 concentrations rapidly decreased with the increase of $PM_{2.5}$ concentrations. In contrast, when the concentrations of $PM_{2.5}$ were greater than 100 $\mu g/m^3$, O_3 concentrations slowly decreased with the increase of $PM_{2.5}$ concentrations. This is consistent with the result of Bian et al (2007).

It is interesting to note that during late spring, summer, and early fall periods, the correlation between $PM_{2.5}$ and O_3 concentrations was positive relationship compared to the negative relationship in winter (see Fig. 3b). This result suggests that O_3 production was high during the heavy haze period, despite the solar radiation was

greatly depressed. In order to clearly display this unusual event, we illustrate diurnal variations of $PM_{2.5}$ and O_3, and NO_2 during a fall period (from Oct.5 to Oc. 6, 2015). Figure 4 shows that during this period (as a case study), the $PM_{2.5}$ concentrations were very high, ranging from 150 to 320 $\mu g/m^3$. Under such high aerosol condition, the solar radiation should be significantly reduced, and O_3 photochemical production would be reduced. However, the diurnal variation of O_3 was unexpectedly strong, with high noontime concentration of >220 $\mu g/m^3$ and very low nighttime concentration of ~25 $\mu g/m^3$. This strong diurnal variation was due to the photochemical activity, which suggested that during relatively low solar conditions, the photochemical activities of O_3 production was high. According to the theory of the O_3 chemical production, the high O_3 production is related to high oxidant of OH (Seinfeld and Pandis, 2006), which should not be occurred during lower solar radiation. This result brings important issue for air pollution control strategy, because the both air pollutants (high $PM_{2.5}$ and O_3) were important air pollution problems in eastern China.

To clearly understand the effect of the high aerosol concentrations on solar radiation, we investigate the meteorological conditions, such as cloud covers, relation humidity (RH), and solar radiation during the period of the case study (see Figs. 5 and 6). Figure 5 shows that the cloud condition was close to the cloud free condition，but there was a very heavy aerosol layer in the Beijing region, suggesting that cloud cover played a minor role in the reduction of the solar radiation. The measured RH values (not shown) were generally higher than 60%, with a maximum of 95% during the period. As a result, the high aerosol concentrations companied by high RH produced important effects on solar radiation. As shown in Fig. 6, the daytime averaged solar radiation was significantly reduced (about 40% reduction in Oct. 5-6 period compared with the value of Oct. 8).

XUEXI TIE 9/7/19 4:26 PM
已设置格式: 字体:12 pt

XUEXI TIE 9/7/19 4:28 PM
已设置格式: 字体:12 pt

XUEXI TIE 9/7/19 4:28 PM
已设置格式: 字体:12 pt

XUEXI TIE 9/7/19 4:30 PM
已设置格式: 字体:12 pt

XUEXI TIE 9/7/19 4:30 PM
已设置格式: 字体:12 pt

2. Method

In order to better understand the O_3 chemical production occurred in heavy aerosol condition in eastern China, the possible O3 production in such condition is discussed. Ozone photochemical production ($P[O_3]$) is strongly related to the amount of OH radicals (Chameides et al., 1999). According to the traditional theory, the amount of surface OH radicals is proportional to the surface of solar radiation, which is represented by

$$[OH] = P[HOx]/L[HOx]^* \qquad \text{(R-1)}$$

Where [OH] represents the concentration of hydroxyl radicals (#/cm^3); HOx represents the concentration of HO_2 + OH (#/cm^3); P[HOx] represents the photochemical production of HOx (#/cm^3/s); and L[HOx]* (1/s) represents the photochemical destruction of HOx, which is normalized by the concentrations of OH.

The major process for the photochemical production of P[HOx] is through the O_3 photolysis and follows by the reaction with atmospheric water vapor. It can express by

$$P[HOx] = J_1[O_3]/(k_1 \times am) \times 2.0 \times k_2[H_2O] = P_1[HOx] \qquad \text{(R-2)}$$

Where J_1 represents the photolysis of $O_3 + h\nu \rightarrow O^1D$; k_1 represents the reaction rate of $O^1D + am \rightarrow O^3P$; and k_2 represents the reaction rate of $O^1D + H_2O \rightarrow 2OH$. As we can see, this HOx production is proportional to the magnitude of solar radiation (J_1), and J_1 is the O_3 photolysis with the solar radiation. Figure 7 shows the relationship between the values of J_1 and aerosol concentrations in October at middle-latitude calculated by the TUV model (Madronich and Flocke, 1999). This result suggests that under the high aerosol concentrations (AOD = 2.5), the J_1 value is strongly depressed, resulting in significant reduction of OH concentrations and O_3 production. For example, the maximum J_1 value is about 2.7×10^{-5} (1/s) with lower aerosol values (AOD = 0.25). According to the previous study, the surface $PM_{2.5}$

XUEXI TIE 9/7/19 4:43 PM
已删除: e

XUEXI TIE 9/7/19 4:44 PM
已删除: (OH)

XUEXI TIE 10/7/19 9:46 AM
已删除: 5

XUEXI TIE 9/7/19 4:45 PM
已删除: (

concentrations were generally smaller than 50 $\mu g/m^3$ with this AOD value (Tie et al., 2017). However, when the AOD value increase to 2.5 (the $PM_{2.5}$ concentrations are generally >100 $\mu g/m^3$), the maximum J_1 value rapidly decreases to about $6x10^{-6}$ (1/s), which is about 450% reduction compared to the value with AOD=0.25. This study suggests that under high $PM_{2.5}$ concentrations (>100 $\mu g/m^3$), the photochemical production of OH (P[HOx]) is rapidly decreased, leading to low OH concentrations, which cannot initiate the high oxidation of O_3 production. As a result, the high O_3 production shown in Fig. 4 cannot be explained. Other sources for O_3 oxidation are needed to explain this result.

Recent studies show that the HONO concentrations are high in eastern China (Huang et al., 2017). Because under high solar radiation, the photolysis rate of HONO is very high, resulting in very low HONO concentrations in daytime (Seinfeld and Pandis, 2006). These measured high HONO concentrations are explained by their studies. One of the explanations is that there are high surface HONO sources during daytime, which produces high HONO concentrations (Huang et al., 2017). Shi et al. (2015) suggest that there are several potential HONO sources, including surface emissions, conversion of NO_2 at the ocean surface, etc. Zhang et al. (2016) parameterized these potential HONO sources in the WRF-Chem model, and the calculated HONO concentrations are increased in the WRF-Chem model. In our calculation, we only use the classical gas-phase chemistry to calculate HONO concentrations, and to illustrate that the importance of these missing sources for the production of OH radicals. Adding these missing sources (there are not fully understand and remain a large uncertainty) could be a very important future work.

Figure 8 shows the measured HONO concentrations in three large cities in China (Shanghai, Xi'an, and Beijing) during fall and winter. It shows that the measured HONO concentrations were high, with a maximum concentration of 2.3 ppbv during morning, and about 0.5-1.0 ppbv in daytime. As a result, we think that the high HONO is a common event in large cities in eastern China, especially in daytime. This

XUEXI TIE 4/7/19 10:52 AM
已设置格式: 字体:12 pt

XUEXI TIE 10/7/19 9:46 AM
已删除: 6

XUEXI TIE 9/7/19 4:03 PM
已删除: two

XUEXI TIE 9/7/19 4:03 PM
已删除: and

XUEXI TIE 9/7/19 4:03 PM
已删除: time

XUEXI TIE 9/7/19 4:07 PM
已设置格式: 字体:12 pt

high HONO is also measured by previous studies (Zhang et al. 2016; Huang et al. 2017). In this study, we make an assumption that the co-occurrence between O_3 and $PM_{2.5}$ occurred under high HONO concentrations. We note that using this assumption may result in some uncertainties in estimating the effect of HONO on OH. For example, using the measured HONO in Xi'an and Beijing could produce 1-2 times higher OH production by photolysis of HONO than the result by using the data from Shanghai. In this case, we use the measured HONO from Shanghai to avoid the over estimate of the HONO effect, which can be considered as a low-limit estimation.

It is also interesting to note that the high HONO concentrations were occurred during high aerosol concentration periods. Figure 9 illustrates that when the $PM_{2.5}$ concentrations increased to 70-80 $\mu g/m^3$, and the HONO concentrations enhanced to 1.4-18 ppbv during September in Shanghai. This measured high HONO concentrations were significantly higher than the calculated concentrations (shown in Fig. 8), suggesting that some additional sources of HONO are needed. This result is consistent with the HONO measurements in other Chinese cities (Huang et al. 2017).

Under the high HONO concentrations in daytime, HONO can be photolyzed to be OH, and become another important process to produce OH. As a result, the OH production rate (P[HOx]) can be written to the following reactions.

$$P_2[HOx] = J_2 \times [HONO] \quad \text{(R-3)}$$

$$P[HOx] = P_1[HOx] + P_2[HOx]$$

$$= J_1[O_3]/(k_1 \times am) \times 2.0 \times k_2[H_2O] + J_2 \times [HONO] \quad \text{(R-4)}$$

Because the chemical lifetime of OH is less than second, OH concentrations can be calculated according to equilibrium of chemical production and chemical loss. With the both OH chemical production processes, the OH concentrations can be calculated by the following equation (Seinfeld and Pandis, 2006).

XUEXI TIE 9/7/19 4:08 PM
已设置格式: 字体:12 pt, 下标

XUEXI TIE 9/7/19 4:07 PM
已设置格式: 字体:12 pt

XUEXI TIE 9/7/19 4:08 PM
已设置格式: 字体:12 pt, 下标

XUEXI TIE 9/7/19 4:07 PM
已设置格式: 字体:12 pt

XUEXI TIE 9/7/19 4:07 PM
已设置格式: 字体:12 pt

XUEXI TIE 9/7/19 4:07 PM
已设置格式: 字体:12 pt

XUEXI TIE 9/7/19 4:07 PM
已设置格式: 字体:12 pt

XUEXI TIE 9/7/19 4:07 PM
已设置格式: 字体:12 pt

XUEXI TIE 9/7/19 4:07 PM
已设置格式: 字体:12 pt

XUEXI TIE 9/7/19 4:07 PM
已设置格式: 字体:12 pt

XUEXI TIE 10/7/19 9:48 AM
已删除: 7

XUEXI TIE 10/7/19 9:48 AM
已删除: 6

$$P1 + P2 = L1 + L2$$

Where P1 and P2 are the major chemical productions, expressed in R-4, and L1 and L2 are the major chemical loss of OH, and represent by

$$L1: \quad OH + NO_2 \rightarrow HNO_3 \qquad (R\text{-}5)$$

$$L2: \quad HO_2 + HO_2 \rightarrow H_2O_2 + O_2 \qquad (R\text{-}6)$$

Under high NOx condition, such as in the Shanghai region, NOx concentrations were often higher to 50 ppbv (shown in Fig. 3), the L1 term is larger than L2. The OH concentrations can be approximately expressed by

$$[HO] = \{J_1[O_3]/(k_1 \times am) \times 2.0 \times k_2[H_2O] + J_2 \times [HONO]\}/ k_3[NO_2] \qquad (R\text{-}5)$$

Where k_3 is the reaction coefficient of $OH + NO_2 \rightarrow HNO_3$.

3. Result and analysis

3.1. OH productions in different HONO conditions

In order to quantify the individual effects of these two OH production terms (P1 and P2) on the OH concentrations, the P1 and P2 are calculated under different daytime HONO conditions (calculated low HONO and measured high HONO concentrations). Figure 10 shows that under the low HONO condition, the P1 is significantly higher than P2, and P2 has only minor contribution to the OH values. For example, the maximum of P1 occurred at 13 pm, with a value of 65×10^6 #/cm^3/s. In contrast, the maximum of P2 occurred at 10 am, with a value of 15×10^6 #/cm^3/s. However, under high HONO condition, the P2 plays very important roles for the OH production. The maximum of P1 occurred at 11 am, with a value of 350×10^6 #/cm^3/s, which is about

XUEXI TIE 10/7/19 9:49 AM
已删除: 8

XUEXI TIE 9/7/19 4:48 PM
已删除: 1

XUEXI TIE 9/7/19 4:48 PM
已删除: 15

500% higher than the P1 value. It is important to note that this calculation is based on the high aerosol condition (AOD = 2.5) in September. This result can explain the high O_3 chemical production in Fig. 4.

3.2. OH in different aerosol conditions

In order to understand the effect of aerosol conditions, especially high aerosol conditions, on the OH concentrations. Figure 11 shows the OH concentrations with and without HONO production of OH. With including the HONO production (i.e., including P1 and P2), the calculated OH concentrations are significantly higher than without including this production (i.e., only including P1). The both calculated OH concentrations are rapidly changed with different levels of aerosol conditions. For example, without HONO production, the maximum OH concentration is about 7.5×10^5 #/cm^3 under low aerosol condition (AOD=0.25). In contrast, the maximum OH concentration rapidly reduced to 1.5×10^5 #/cm^3 under high aerosol condition (AOD=2.5), and further decreased to 1.0×10^5 #/cm^3 with the AOD value of 3.5. In contrast, with including HONO production, the OH concentrations significantly increased. Under higher aerosol condition (AOD=2.5), the maximum of OH concentration is about 7.5×10^5 #/cm^3, which is the same value under low aerosol condition in the no-HONO case. This result suggests that the measured high O_3 production occurred in the high aerosol condition is likely due to the high HONO concentrations in Shanghai.

XUEXI TIE 10/7/19 9:49 AM
已删除: 9

3.3. Effects of clouds

Cloud cover can have very important impacts on the photolysis of HONO, which can affect the effect of HONO on the OH radicals. The above calculations are based on the cloud-free condition, with heavy aerosol concentration in the Beijing region. As shown in Fig. 5, during the case study period (Oct 5 to 6, 2015) (see Fig. 4), the weather map shows that the cloud-free condition, with heavy aerosol condition.

In order to understand the effects of cloud on the photolysis of HONO, we include different cloud covers in the TUV model. The calculated results show in Fig. 12. The results show that the thin cloud (with cloud cover in 2 km and cloud water of 10 g/m^3), could reduce the photolysis rate of HONO by about 40%, but the HONO could still remain important effects. However, with dense cloud condition (with cloud covers at 2 and 3 km and cloud water of 50 10 g/m^3), the photolysis rate of HONO could reduce by 9-10 times by the cloud. In this case, adding photolysis rate of HONO cannot produce important effect on OH radicals and the production of O_3.

XUEXI TIE 4/7/19 11:05 AM
已设置格式: 字体:12 pt

XUEXI TIE 4/7/19 11:05 AM
已设置格式: 字体:12 pt

XUEXI TIE 4/7/19 11:05 AM
已设置格式: 字体:12 pt

XUEXI TIE 4/7/19 11:03 AM
已删除:

3.3. OH in winter

The measurement of O_3 also shows that the concentrations in winter were always low (see Fig. 2), suggesting that the O_3 concentrations were not significantly affected by the appearance of HONO. Figure 10 shows the OH concentrations in September and December. It shows that under different aerosol conditions, OH concentrations in December were very low compared with the values in September. Both the calculated OH concentrations include the HONO production term. For example, under the condition of AOD=2.5, the maximum OH is about 7.5×10^5 #/cm^3 in September, while it rapidly reduces to 1.5×10^5 #/cm^3 in December. Under the condition of AOD=3.5, the maximum OH is still maintaining to a relative high level (4.5×10^5 #/cm^3) in September. However, the maximum OH values are extremely low in December, with maximum value of 0.5×10^5 #/cm^3 in December. Because both the OH chemical productions (P1 and P2) are strongly dependent upon solar radiation (see equation R-4), the seasonal variation of solar radiation plays important roles for controlling the OH production in winter (see Fig. 13). Because the solar radiation is in a very low level in winter, adding the photolysis of HONO has smaller effect in winter than in fall, and OH remains low values by including the HONO production term.

XUEXI TIE 9/7/19 4:36 PM
已删除: When

XUEXI TIE 9/7/19 4:43 PM
已删除: it reaches a threshold level to prevent the OH chemical production, even

Summary

689 Currently, China is undergoing a rapid economic development, resulting in a high
690 demand for energy, greater use of fossil fuels. As a result, the high emissions of
691 pollutants produce heavy aerosol pollutions ($PM_{2.5}$) in eastern China, such as in the
692 mega city of Beijing. The long-term measurements show that in addition to the heavy
693 aerosol pollution, the O_3 pollution becomes another major pollutants in the Beijing
694 region. The measured results show that there were very strong seasonal variation in
695 the concentrations of both $PM_{2.5}$ and O_3 in the region. During winter, the seasonal
696 variability of O_3 concentrations were anti-correlated with the $PM_{2.5}$ concentrations.
697 However, during late spring and fall periods, the correlation between $PM_{2.5}$ and O_3
698 concentrations was positive compared to the negative in winter. This result suggests
699 that during heavy aerosol condition (the solar radiation was depressed), the O_3
700 chemical production was still high, appearing a double peak of $PM_{2.5}$ and O_3 during
701 fall period. This co-occurrence of high $PM_{2.5}$ and O_3 is the focus of this study. The
702 results are highlighted as follows;
703
704 (1) There are high daytime HONO concentrations in major Chinese mega cities, such
705 as in Beijing and Shanghai. It is also interesting to note that the high HONO
706 concentrations were occurred during high aerosol concentration periods. Under
707 the high daytime HONO concentrations, HONO can be photo-dissociated to be
708 OH radicals, and becomes an important process to produce OH.
709 (2) With including the OH production of measured HONO concentrations, the
710 calculated OH concentrations are significantly higher than without including this
711 production. For example, without HONO production, the maximum OH
712 concentration is about 7.5×10^5 #/cm^3 under low aerosol condition (AOD=0.25),
713 and rapidly reduced to 1.5×10^5 #/cm^3 under high aerosol condition (AOD=2.5) in
714 September. In contrast, by including HONO production, the OH concentrations
715 significantly increased. For example, under higher aerosol condition (AOD=2.5),
716 the maximum of OH concentration is about 7.5×10^5 #/cm^3, which is similar to the
717 value under low aerosol condition in the no-HONO case. This result suggests that
718 even under the high aerosol conditions, the chemical oxidizing process for O_3

production can be active. This result is likely for explaining the co-occurrence of high $PM_{2.5}$ and high O_3 in fall season in eastern China.

(3) The measurement of O_3 also shows that the concentrations in winter were always low, suggesting that the O_3 concentrations were not significantly affected by the appearance of HONO. The calculated result shows that the seasonal variation of solar radiation plays important roles for controlling the OH production in winter. Because the solar radiation is in a very low level in winter, adding the photolysis of HONO has smaller effect in winter than in fall, and OH remains low values by including the HONO production term.

Because in recent years, the $PM_{2.5}$ pollutions are reduced due to the large control efforts by the Chinese government, the O_3 pollutions become another severe pollution problem in eastern China. This study is important, because it provides some important scientific highlights to better understand the O_3 pollutions in eastern China.

Author contributions. XT came up with the original idea of investigating the scientific issue. XT and JX designed the analysis method. XL, GL and SZ provided the observational data and helped in discussion. XT prepared the manuscript with contributions from all co-authors.

Acknowledgement

This work was supported by the National Natural Science Foundation of China (NSFC) under Grant Nos. 41430424 and 41730108. The Authors thanks the supports of Center for Excellence in Urban Atmospheric Environment, Institute of Urban Environment, Chinese Academy of Sciences.

XUEXI TIE 9/7/19 4:49 PM

已删除: When the solar radiation is a very low level in winter, it reaches a threshold level to prevent the OH chemical production, even by including the HONO production term.

XUEXI TIE 10/7/19 10:01 AM

已删除: The National Center for Atmospheric Research is sponsored by the National Science Foundation.

References

Bian H., S.Q. Han, X. Tie, M.L. Shun, and A.X. Liu, Evidence of Impact of Aerosols on Surface Ozone Concentration: A Case Study in Tianjin, China, *Atmos. Environ*., *41, 4672-4681,* 2007.

Chameides, W. L., Fehsenfeld, F., Rodgers, M. O., Cardelino, C., Martines, J., Parrish, D., Lonneman, W., Lawson, D. R., Ras- mussen, R. A., Zimmerman, P., Greenberg, J., Middleton, P., and Wang, T.: Ozone precursor relationships in the ambient atmo- sphere, *J. Geophys. Res., 97*, 6037–6055, 1992.

Deng X.J, X Tie, D. Wu, XJ Zhou, HB Tan, F. Li, C. Jiang, Long-term trend of visibility and its characterizations in the Pearl River Delta Region (PRD), China, *Atmos. Environ*., *42,* 1424-1435*,* 2008.

Geng, F.H., C.S., Zhao, X. Tang, GL. Lu, and X. Tie, Analysis of ozone and VOCs measured in Shanghai: A case study, *Atmos. Environ*., *41*, 989-1001, 2007.

Geng, FH, CG Cai, X. Tie, Q. Yu, JL An, L. Peng, GQ Zhou, JM Xu, Analysis of VOC emissions using PCA/APCS receptor model at city of Shanghai, China, *J. Atmos. Chem.,* 62, 229–247, DOI :10.1007/s10874-010-9150-5, 2010.

He, S., & Carmichael, G. R. (1999). Sensitivity of photolysis rates and ozone production in the troposphere to aerosol properties. Journal of Geophysical Research: Atmospheres, 104(D21), 26307-26324.

Huang, J.P, X. Y. Liu, C. Y. Li, L. Ding, H. P. Yu, The global oxygen budget and its future projection. *Science Bull. 63,* 1180–1186, 2018.

Huang J., Y. Li, C. Fu, F. Chen, Q. Fu, A. Dai, M. Shinoda, Z. Ma, W. Guo, Z. Li, L. Zhang, Y. Liu, H. Yu, Y. He, Y. Xie, X. Guan , M. Ji, L. Lin, S. Wang, H. Yan and G. Wang, Dryland climate change recent progress and challenges. *Rev. of Geophys., 55,* 719-778, doi:10.1002/2016RG000550, 2017.

Huang, R. J., L. Yang, JJ Cao, QY Wang, X. Tie, et al., Concentration and sources of atmospheric nitrous acid (HONO) at an urban site in Western China. *Sci. of Total Environ*., 593-594, 165-172, doi.org/10.1016/j.scitotenv.2017.02.166, 2017.

Lei, W., R. Zhang, X. Tie, P. Hess, Chemical characterization of ozone formation in the Houston-Galveston area, *J. Geophys. Res., 109,* doi:10.102/2003JD004219, 2004.

Li, G., Bei, N., Cao, J., Wu, J., Long, X., Feng, T., Dai, W., Liu, S., Zhang, Q., and Tie, X.: Widespread and persistent ozone pollution in eastern China during the

XUEXI TIE 2/7/19 5:19 PM
已设置格式: 字体:12 pt

XUEXI TIE 2/7/19 5:19 PM
已设置格式: 缩进: 悬挂缩进: 2.02 字符, 左 -0.01 字符, 首行缩进: -2.02 字符, 定义网格后自动调整右缩进, 调整中文与西文文字的间距, 调整中文与数字的间距

XUEXI TIE 2/7/19 5:19 PM
已设置格式: 字体颜色: 文字 1

non-winter season of 2015: observations and source attributions, *Atmos. Chem. Phys., 17*, 2759-2774, doi:10.5194/acp-17-2759-2017, 2017.

Long, X., X. Tie, JJ Cao, RJ Huang, T. Feng, N. Li, SY Zhao, J. Tian, GH Li, Q. Zhang, Impact of crop field burning and mountains on heavy haze in the North China Plain: A case study, *Atmos. Chem. Phys.,* 16, 9675-9691, doi:10.5194/acp-16-9675-2016, 2016.

Madronich, S. & Flocke, S. in *Environmental Photochemistry* 2 / 2L, 1–26 (Springer Berlin Heidelberg, 1999)

Quan, J.N., Y. Gao, Q. Zhang, X. Tie*, JJ Cao, SQ Han, JW Meng, PF Chen, DL Zhao, Evolution of Planetary Boundary Layer under different weather conditions, and its impact on aerosol concentrations, *Particuology*, doi: 10.1016/j.partic.2012.04.005, 2013.

Seinfeld, J. H. and Pandis, S. N.: *Atmospheric Chemistry and Physics*: From Air Pollution to Climate Change, 2nd Edn., John Wiley and Sons, New York, 2006.

Shi, C., Wang, S., Liu, R., Zhou, R., Li, D., Wang, W., ... & Zhou, B. (2015). A study of aerosol optical properties during ozone pollution episodes in 2013 over Shanghai, China. Atmospheric Research, 153, 235-249.

Sillman, S.: The use of NO_y , H_2O_2, and HNO_3 as indicators for ozone-NO_x-hydrocarbon sensitivity in urban locations, J. Geo- phys. Res., 100, 14175–14188, 1995.

Tie, X., G. Brasseur, C. Zhao, C. Granier, S. Massie, Y. Qin, P.C. Wang, GL Wang, PC, Yang100,, Chemical Characterization of Air Pollution in Eastern China and the Eastern United States, *Atmos. Environ., 40*. 2607-2625, 2006.

Tie, X., D. Wu, and G. Brasseur, Lung Cancer Mortality and Exposure to Atmospheric Aerosol Particles in Guangzhou, China, *Atmos. Environ*, 43, 2375–2377, 2009a.

Tie, X., FH. Geng. L. Peng, W. Gao, and CS. Zhao, Measurement and modeling of O_3 variability in Shanghai, China; Application of the WRF-Chem model, *Atmos. Environ., 43,* 4289-4302, 2009b.

Tie X., F. Geng, A. Guenther, J. Cao, J. Greenberg, R. Zhang, E. Apel, G. Li, A. Weinheimer, J. Chen, and C. Cai, Megacity impacts on regional ozone formation: observations and WRF-Chem modeling for the MIRAGE-Shanghai field campaign, *Atmos. Chem. Phys., 13*, 5655-5669, doi:10.5194/acp-13-5655-2013, 2013.

XUEXI TIE 2/7/19 5:18 PM
已设置格式: 字体:12 pt

XUEXI TIE 2/7/19 5:18 PM
已设置格式: 左, 缩进: 左: 0 cm, 悬挂缩进: 1.77 字符, 首行缩进: -1.77 字符, 行距: 单线, 孤行控制

XUEXI TIE 2/7/19 5:18 PM
已删除:

XUEXI TIE 2/7/19 5:18 PM
已设置格式: 字体颜色: 文字 1

827 Tie, X., Q. Zhang, H. He, JJ Cao, SQ Han, Y. Gao, X. Li, and XC Jia, A budget
828 analysis on the formation of haze in Beijing, *Atmos. Environ*., 25-36, 2015.

829 Tie, X., RJ Huang, WT Dai, JJ Cao, X. Long, XL Su, SY Zhao, QY Wang, GH Li,
830 Effect of heavy haze and aerosol pollution on rice and wheat productions in China,
831 *Sci. Rep.* 6, 29612; doi: 10.1038/srep29612, 2016.

832 Tie, X., J.J. Cao, Understanding Variability of Haze in Eastern China, *J Fundam*
833 *Renewable Energy Appl, 7*:6 DOI: 10.4172/2090-4541.100024, 2017.

834 Tie, X., R.J. Huang, J.J. Cao, Q. Zhang, Y.F. Cheng, H. Su, D. Chang, U. Pöschl, T.
835 Hoffmann, U. Dusek, G. H. Li, D. R. Worsnop, C. D. O'Dowd, Severe Pollution
836 in China Amplified by Atmospheric Moisture, *Sci. Rep.* 7: 15760 |
837 DOI:10.1038/s41598-017-15909-1, 2017.

838 Zhang, L., Wang, T., Zhang, Q., Zheng, J., Xu, Z., & Lv, M., Potential sources of
839 nitrous acid (HONO) and their impacts on ozone: A WRF/Chem study in a
840 polluted subtropical region. Journal of Geophysical Research: Atmospheres,
841 121(7), 3645- 3662, 2016.
842
843 Zhang, R., X. Tie, and D. Bond, Impacts of Anthropogenic and Natural NO_x Sources
844 over the U.S. on Tropospheric Chemistry, *Proceedings of National Academic*
845 *Science USA*, *100,* 1505-1509, 2003.

846 Zhang, Q., C. Zhao, X. Tie, Q. Wei ,G. Li, and C. Li, Characterizations of Aerosols
847 over the Beijing Region: A Case Study of Aircraft Measurements, 40,
848 4513-4527, *Atmos. Environ.,* 2006.

849
850

XUEXI TIE 2/7/19 5:17 PM
已设置格式: 字体:12 pt

XUEXI TIE 2/7/19 5:17 PM
已设置格式: 缩进: 左: 0 cm, 悬挂缩进: 1.77 字符, 首行缩进: -1.77 字符, 定义网格后自动调整右缩进, 空格 段后: 0 pt, 调整中文与西文文字的间距, 调整中文与数字的间距

XUEXI TIE 2/7/19 5:17 PM
已设置格式: 字体:12 pt

XUEXI TIE 2/7/19 5:17 PM
已设置格式: 字体:12 pt

XUEXI TIE 2/7/19 5:17 PM
已设置格式: 字体颜色: 文字 1

Figure Caption

Fig. 1. The geographic locations of the measurement sites in Beijing, in which the measured concentrations of $PM_{2.5}$ and O_3 are used to the analysis.

Fig. 2. The daily averaged concentrations of $PM_{2.5}$ and O_3 in the Beijing region in 2015. The concentrations are averaged over all sites shown in Fig. 1. The blue lines represent the $PM_{2.5}$ concentrations ($\mu g/m^3$), and the red bars represent the O_3 concentrations ($\mu g/m^3$). The rectangles show some typical events during winter (green), spring and fall (orange), and summer (red).

Fig. 3. The correlation between O_3 and $PM_{2.5}$ concentrations during winter (upper panel) and during late spring and fall (lower panel). During winter, O_3 concentrations were strong anti-correlated with the $PM_{2.5}$ concentrations. During late spring and fall, O_3 concentrations were correlated with the $PM_{2.5}$ concentrations.

Fig. 4. The diurnal variations of $PM_{2.5}$ (blue line) and O_3 (red line), and NO_2 (green line) during a fall period (from Oct.5 to Oc. 6, 2015). It shows that with high $PM_{2.5}$ condition, there was a strong O3 diurnal variation.

Fig. 5. The cloud condition during the period of the case study (between Oct 5 and 6, 2015) in the Beijing region. The bright white color shows the cloud covers, and the grey white shows the haze covers. The Beijing region was under the heavy haze conditions during the period.

Fig. 6. The measured solar radiation (W/m^2) from Oct. 3 to Oct. 9, 2015 in Beijing. The upper panel shows hourly values, and the lower panel shows the daytime averaged values.

Fig. 7. The effect of aerosol levels with AOD = 0.25 (black line), AOD = 2.5 (red line), AOD = 3.5 (blue line), and AOD = 4.0 (green line) on the O_3 photolysis calculated by the TUV model in October at middle-latitude.

Fig. 8. The measured HONO concentrations (ppbv) in three large cities in China. The red line was measured in Xi'An from 24 July to August 6, 2015. The blue line was measured in Shanghai from 9 to 18 September, 2009. The dark-red line was measured in Beijing from 1 to 27 January, 2014. The green line is calculated by the WRF-Chem model. The measurement in fall of Shanghai is applied to the calculation for the OH production of HONO.

Fig. 9. The measured HONO (upper panel) and $PM_{2.5}$ concentrations (lower panel) in fall in Shanghai. It illustrates that the high HONO concentrations were corresponded with high $PM_{2.5}$ concentrations.

XUEXI TIE 10/7/19 9:53 AM
已设置格式: 字体:12 pt

XUEXI TIE 10/7/19 9:54 AM
已设置格式: 字体:12 pt

XUEXI TIE 10/7/19 9:54 AM
已设置格式: 不对齐到网格

XUEXI TIE 10/7/19 9:54 AM
已删除:

XUEXI TIE 10/7/19 9:53 AM
已设置格式: 字体颜色: 蓝色

XUEXI TIE 10/7/19 9:54 AM
已删除: 5

XUEXI TIE 10/7/19 9:55 AM
已设置格式: 字体:12 pt

XUEXI TIE 10/7/19 9:55 AM
已设置格式: 字体颜色: 蓝色

XUEXI TIE 10/7/19 9:55 AM
已删除:

XUEXI TIE 10/7/19 9:54 AM
已删除: 7

Fig. 10. The calculated OH production P(HOx) (#/cm^3/s) by using the model calculated HONO (low concentrations) (in the upper panel) and by using the measured HONO (high concentrations) (in the lower panel). The red bars represent the calculation of the P1 term, and the red bars represent the calculation of the P2 term (OH production from HONO).

Fig. 11. The calculated OH concentrations (#/cm^3) with (upper panel) and without (lower panel) HONO production of OH, under different aerosol levels. Dark red (AOD=0.25), red (AOD=2.5)), red (AOD=3.5)), and red (AOD=4.0).

Fig 10. The cloud condition during the period of the case study (between Oct 5 and 6, 2015 in the Beijing region. The bright white color shows the cloud covers, and the grey white shows the haze covers. The Beijing region is under the heavy haze conditions during the period.

Fig. 12. The effect of cloud cover on the photolysis rate of HONO (J[HONO]). The blue, red, and green lines represent the cloud water vapor of 0 (cloud-free), 10 (g/m^3 – thin cloud), and 50 (g/m^3 – thick cloud), respectively. The left panel (A) represents the light aerosol condition, with AOD of 0.25, and the right panel (B) represents the heavy aerosol condition, with AOD of 2.5.

Fig. 13. The calculated OH concentrations in September (blue bars) and December (dark red bars), under different aerosol levels.

XUEXI TIE 10/7/19 9:55 AM
已删除: 8

XUEXI TIE 10/7/19 9:56 AM
已删除: 9

XUEXI TIE 4/7/19 11:07 AM
已设置格式: 字体:12 pt

XUEXI TIE 10/7/19 9:56 AM
已设置格式: 字体:12 pt, 加粗

XUEXI TIE 4/7/19 11:07 AM
已设置格式: 字体:12 pt

XUEXI TIE 4/7/19 11:07 AM
已删除: 0

Figures

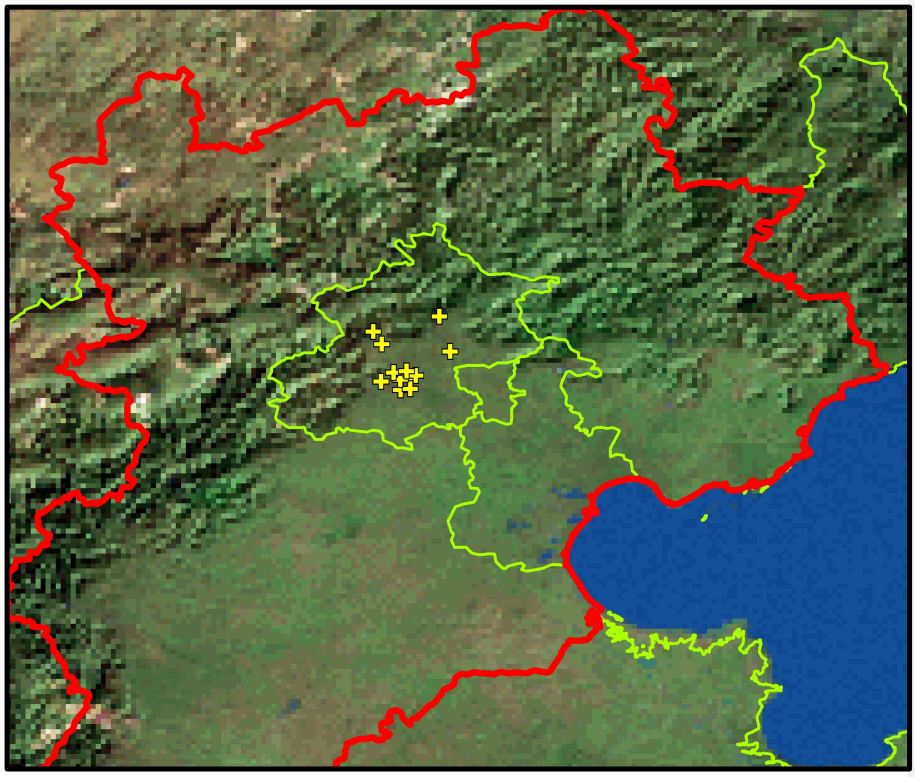

Fig. 1. The geographic locations of the measurement sites in Beijing, in which the measured concentrations of $PM_{2.5}$ and O_3 are used to the analysis.

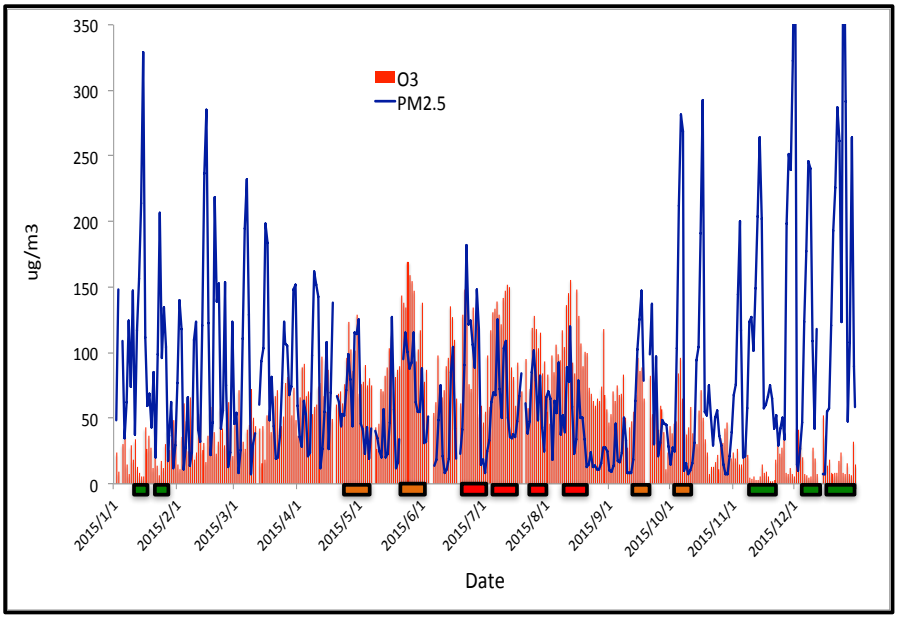

936
937
938 **Fig. 2.** The daily averaged concentrations of $PM_{2.5}$ and O_3 in the Beijing region in 2015. The
939 concentrations are averaged over all sites shown in Fig. 1. The blue lines represent the $PM_{2.5}$
940 concentrations ($\mu g/m^3$), and the red bars represent the O_3 concentrations ($\mu g/m^3$). The rectangles
941 show some typical events during winter (green), spring and fall (orange), and summer (red).
942
943
944
945
946

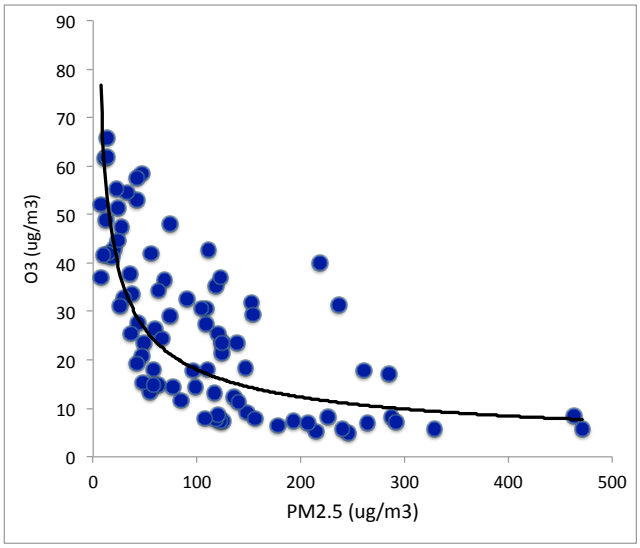

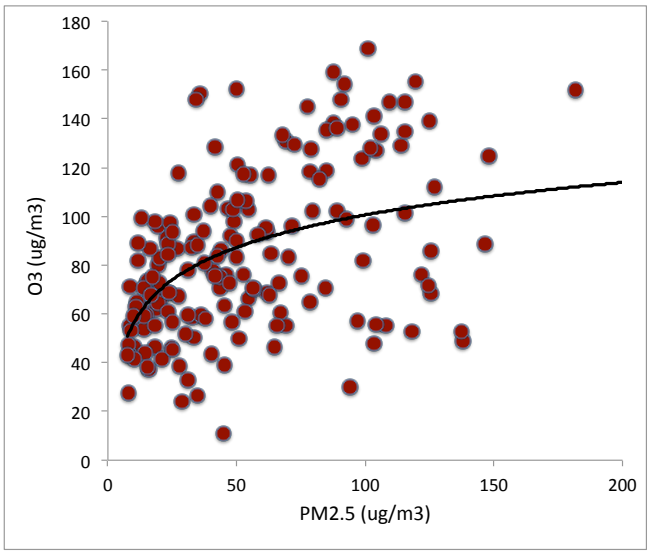

Fig. 3. The correlation between O_3 and $PM_{2.5}$ concentrations during winter (upper panel) and during late spring and fall (lower panel). During winter, O_3 concentrations were strong anti-correlated with the $PM_{2.5}$ concentrations. During late spring and fall, O_3 concentrations were correlated with the $PM_{2.5}$ concentrations.

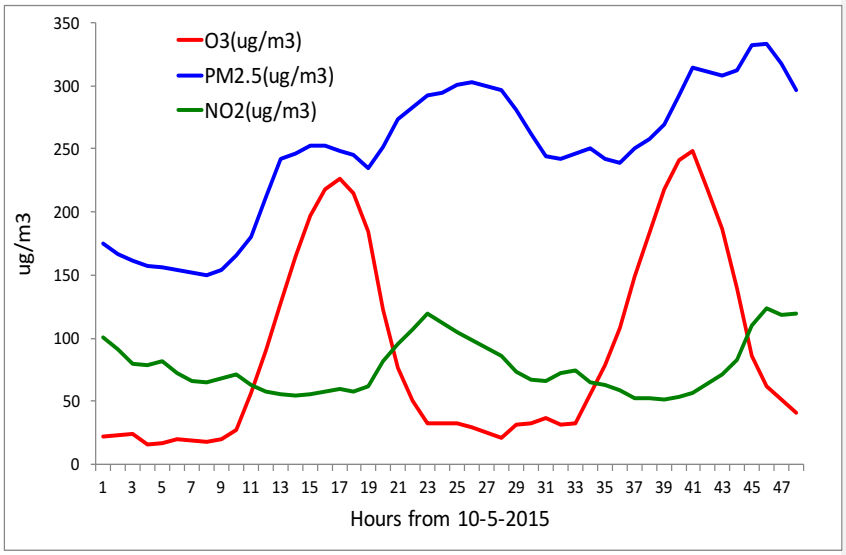

Fig. 4. The diurnal variations of $PM_{2.5}$ (blue line) and O_3 (red line), and NO_2 (green line) during a fall period (from Oct. 5 to Oct. 6, 2015). It shows that with high $PM_{2.5}$ condition, there was a strong O_3 diurnal variation.

XUEXI TIE 4/7/19 10:55 AM
已设置格式: 下标

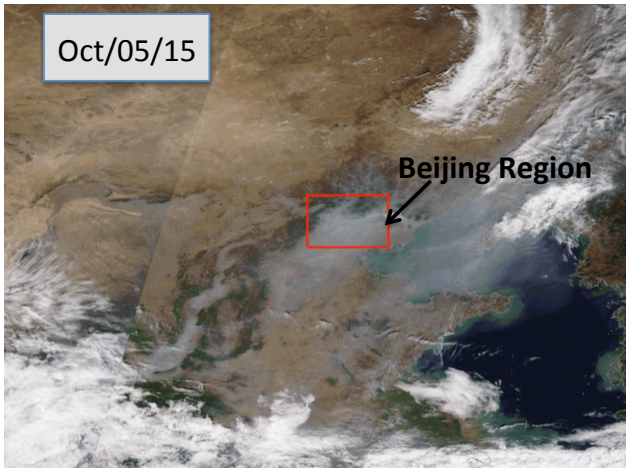

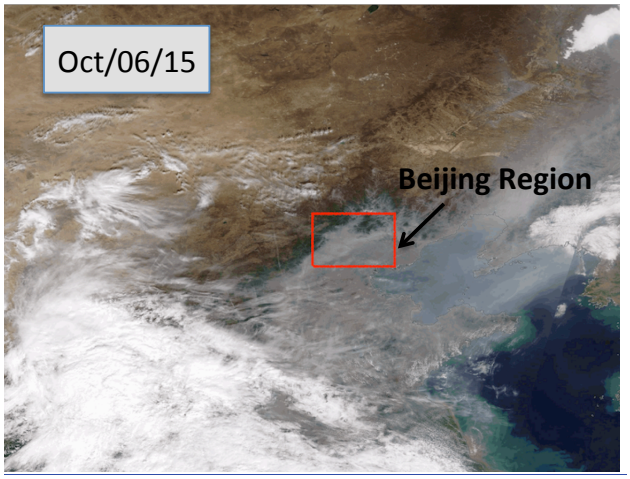

Fig. 5. The cloud condition during the period of the case study (between Oct 5 and 6, 2015 in the Beijing region. The bright white color shows the cloud covers, and the grey white shows the haze covers. The Beijing region is under the heavy haze conditions during the period.

XUEXI TIE 9/7/19 4:21 PM
已设置格式: 缩进: 首行缩进: 6.81 字符

XUEXI TIE 9/7/19 4:22 PM
已设置格式: 字体:加粗

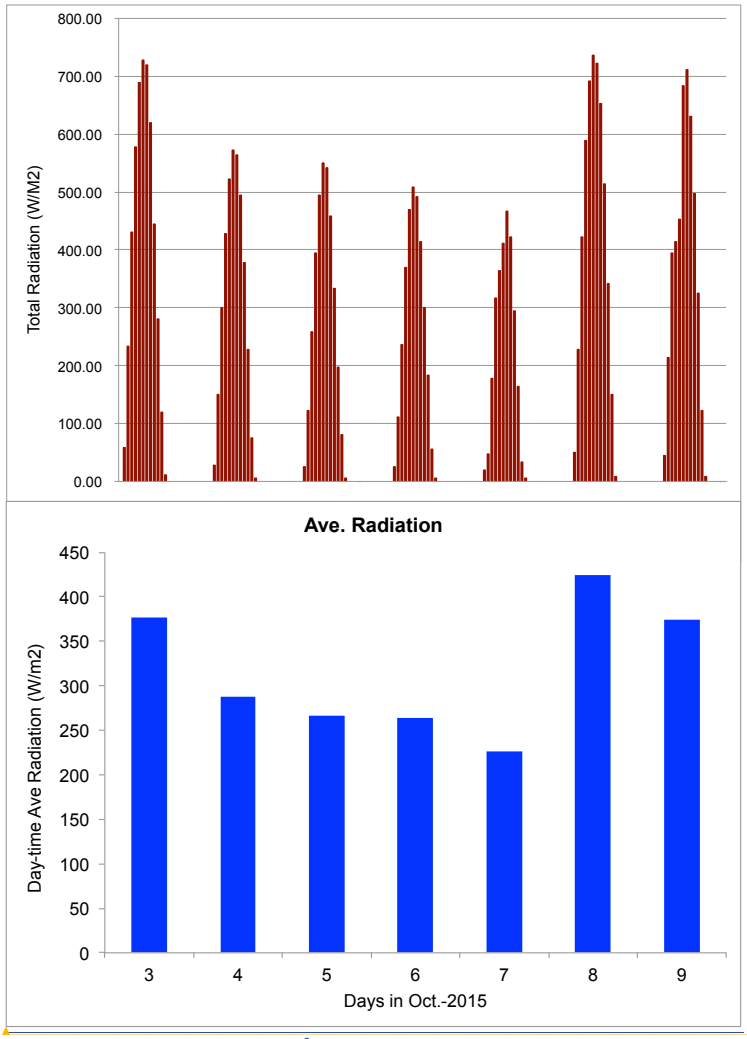

Fig. 6. The measured solar radiation (W/m^2) from Oct. 3 to Oct. 9, 2015 in Beijing. The upper panel shows hourly values, and the lower panel shows the daytime averaged values.

Unknown
已设置格式: 字体:(默认) Times New Roman, 11 pt, 字体颜色: 蓝色

XUEXI TIE 10/7/19 9:22 AM
已设置格式: 缩进: 首行缩进: 4.51 字符

XUEXI TIE 9/7/19 4:32 PM
已设置格式: 字体:加粗

XUEXI TIE 9/7/19 4:22 PM
已设置格式: 缩进: 首行缩进: 6.81 字符

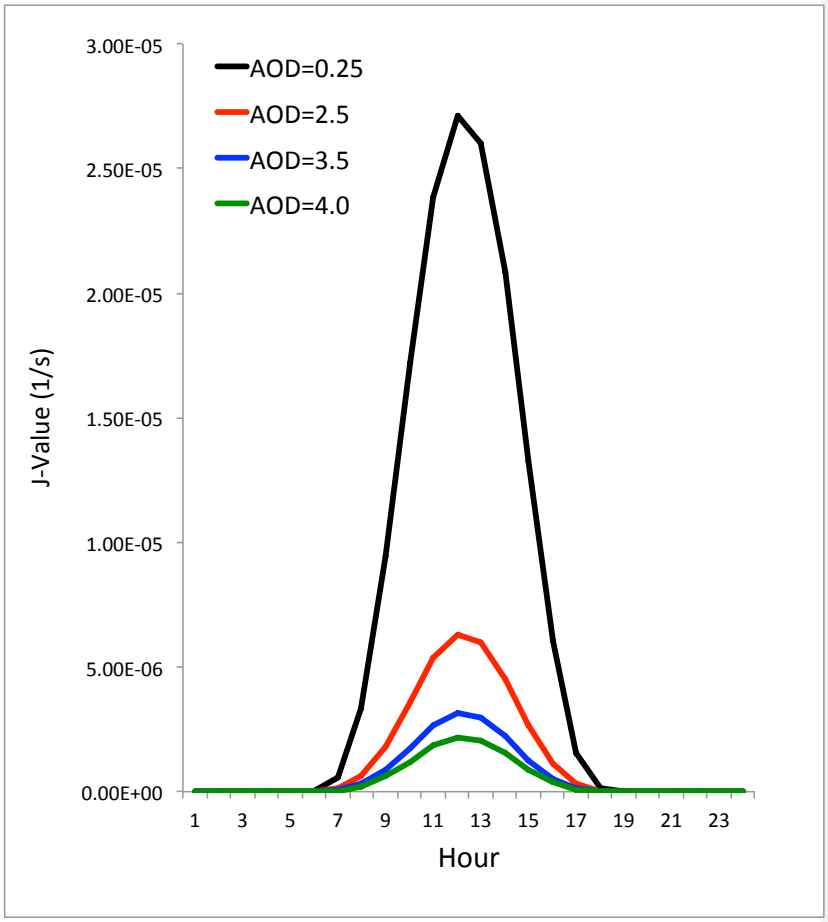

Fig. 7. The effect of aerosol levels with AOD = 0.25 (black line), AOD = 2.5 (red line), AOD = 3.5 (blue line), and AOD = 4.0 (green line) on the O_3 photolysis calculated by the TUV model in October at middle-latitude.

XUEXI TIE 10/7/19 10:28 AM
已删除: 5

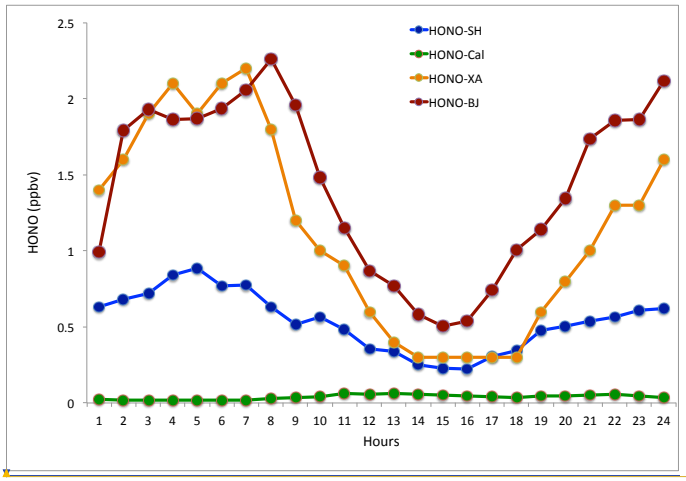

Fig. 8. The measured HONO concentrations (ppbv) in three large cities in China. The red line was measured in Xi'An from 24 July to August 6, 2015. The blue line was measured in Shanghai from 9 to 18 September, 2009. The dark-red line was measured in Beijing from 1 to 27 January, 2014. The green line is calculated by the WRF-Chem model. The measurement in fall of Shanghai is applied to the calculation for the OH production of HONO.

XUEXI TIE 9/7/19 4:00 PM

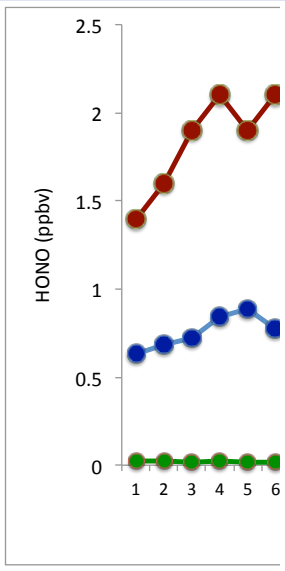

已删除:

Unknown

已设置格式: 字体:(默认) Times New Roman, 字体颜色: 文字 1

Unknown

已设置格式: 字体:(默认) Times New Roman

XUEXI TIE 10/7/19 10:28 AM

已删除: **6**

XUEXI TIE 9/7/19 4:01 PM

已删除: The measured HONO concentrations (ppbv) in two large cities in China. The red line was measured in Xi'An from 24 July to August 6, 2015. The blue line was measure in Shanghai from 9 to 18 September, 2009. The green line is calculated by the WRF-Chem model. The measurement in fall of Shanghai is applied to the calculation for the OH production of HONO.

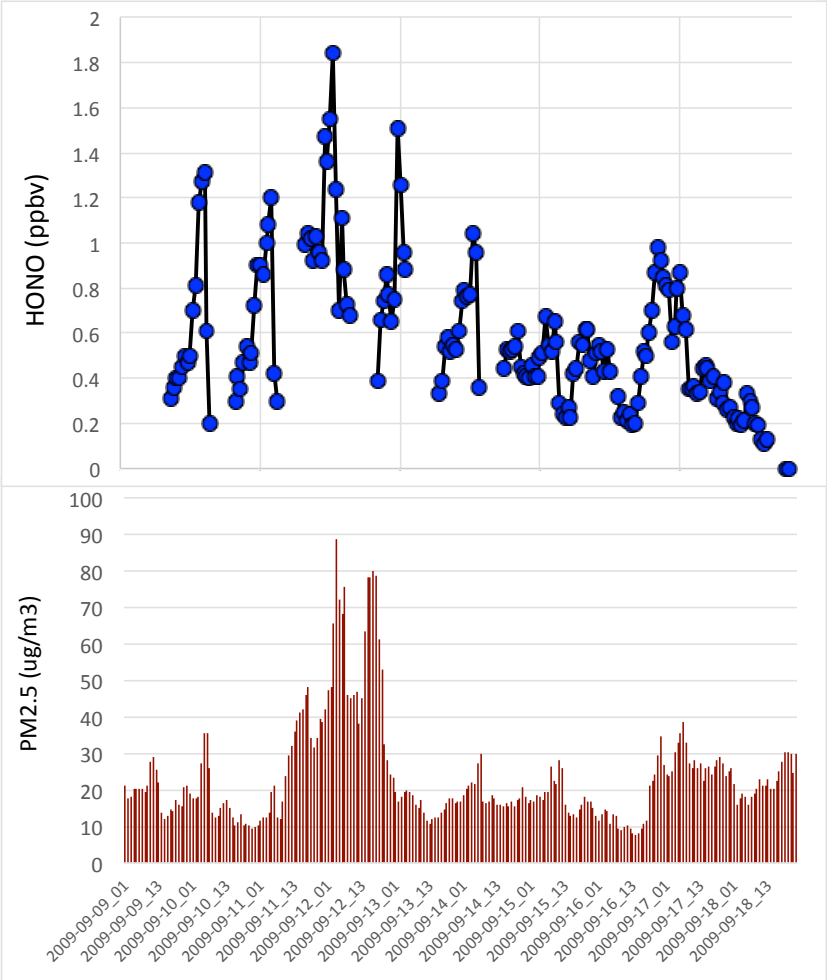

Fig. 9. The measured HONO (upper panel) and $PM_{2.5}$ concentrations (lower panel) in fall in Shanghai. It illustrates that the high HONO concentrations were corresponded with high $PM_{2.5}$ concentrations.

XUEXI TIE 10/7/19 10:28 AM
已删除: 7

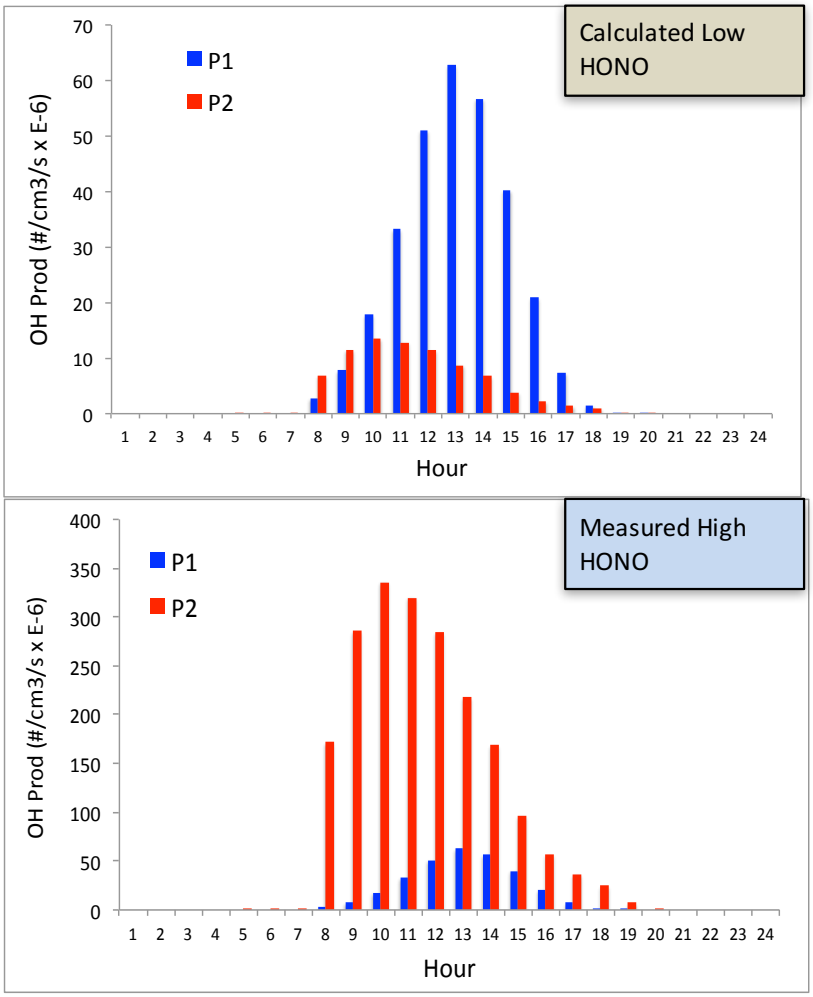

Fig. 10. The calculated OH production P(HOx) (#/cm^3/s) by using the model calculated HONO (low concentrations) (in the upper panel) and by using the measured HONO (high concentrations) (in the lower panel). The red bars represent the calculation of the P1 term, and the red bars represent the calculation of the P2 term (OH production from HONO).

XUEXI TIE 10/7/19 10:28 AM
已删除: 8

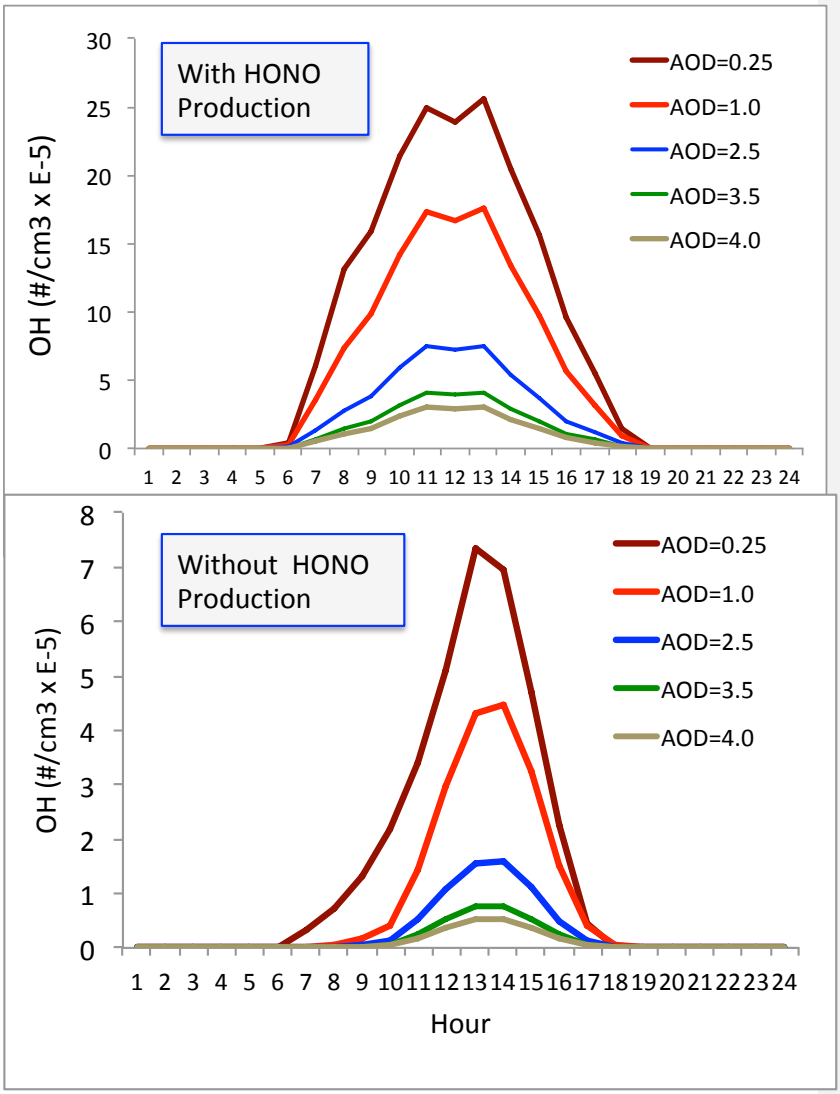

Fig. 11. The calculated OH concentrations (#/cm^3) with (upper panel) and without (lower panel) HONO production of OH, under different aerosol levels. Dark red (AOD=0.25), red (AOD=2.5)), red (AOD=3.5)), and red (AOD=4.0).

XUEXI TIE 10/7/19 10:28 AM
已删除: 9

XUEXI TIE 4/7/19 11:09 AM
已设置格式: 缩进: 首行缩进: 9.45 字符

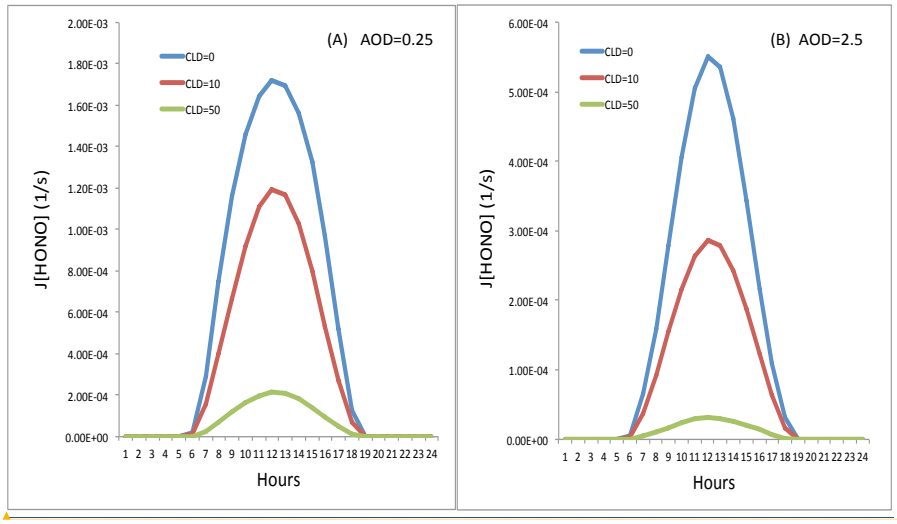

Fig. 12. The effect of cloud cover on the photolysis rate of HONO (J[HONO]). The blue, red, and green lines represent the cloud water vapor of 0 (cloud-free), 10 (g/m^3 – thin cloud), and 50 (g/m^3 – thick cloud), respectively. The left panel (A) represents the light aerosol condition, with AOD of 0.25, and the right panel (B) represents the heavy aerosol condition, with AOD of 2.5.

Unknown
已设置格式: 字体:(默认) Times New Roman

XUEXI TIE 10/7/19 10:29 AM
已设置格式: 字体:加粗

XUEXI TIE 4/7/19 11:09 AM
已设置格式: 缩进: 首行缩进: 4.24 字符

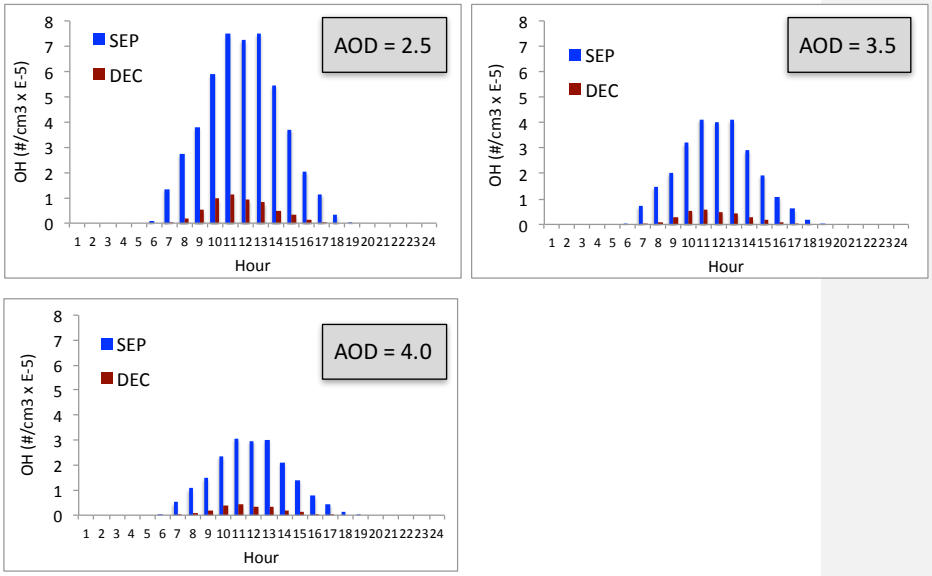

Fig. 13. The calculated OH concentrations in September (blue bars) and December (dark red bars), under different aerosol levels.

XUEXI TIE 4/7/19 11:09 AM
已删除: 0